

ORIGINAL ARTICLE

Loss of a single *Hic1* allele accelerates polyp formation in *Apc*^{Δ716} miceHP Mohammad^{1,4}, W Zhang^{1,4}, HS Prevas¹, BR Leadem¹, M Zhang¹, JG Herman¹, CM Hooker¹, DN Watkins², B Karim³, DL Huso³ and SB Baylin¹¹The Sidney Kimmel Comprehensive Cancer Institute at Johns Hopkins, Johns Hopkins University, Baltimore, MD, USA; ²Centre for Cancer Research, Monash Institute of Medical Research, Monash University, Clayton, Victoria, Australia and ³Department of Molecular and Comparative Pathobiology, Johns Hopkins University, Baltimore, MD, USA

Adenomatous polyposis coli (APC) gene mutations have been implicated in familial and sporadic gastrointestinal (GI) cancers. APC mutations are associated with autosomal dominant inheritance of disease in humans. Similarly, mice that contain a single mutant APC gene encoding a protein truncated at residue 716 (*Apc*^{Δ716}) develop multiple polyps throughout the GI tract as early as 4 weeks after birth. Inactivation of another tumor suppressor gene, *Hypermethylated in Cancer 1 (HIC1)*, often occurs in human colon cancers, among others, via CpG island hypermethylation. Homozygous deletion of *Hic1* in mice results in major developmental defects and embryonic lethality. *Hic1* heterozygotes have previously been shown to develop tumors of a variety of tissue types. We now report that loss of a single *Hic1* allele can promote crypt hyperplasia and neoplasia of the GI tract, and *Hic1*^{+/-}, *Apc*^{+/Δ716} double heterozygotes (DH) develop increased numbers of polyps throughout the GI tract at 60 days. *Hic1* expression is absent in polyps from DH mice, with concomitant increased expression of two transcriptional repression targets of *Hic1*, *Sirt1* and *Sox9*. Together, our data suggest that loss of a gene frequently silenced via epigenetic mechanisms, *Hic1*, can cooperate with loss of a gene mutated in GI cancer, *Apc*, to promote tumorigenesis in an *in vivo* model of multiple intestinal neoplasia.

Oncogene (2011) 30, 2659–2669; doi:10.1038/onc.2010.633; published online 7 February 2011

Keywords: *Hic1*; *Min*; Polyp; DNA hypermethylation; colon cancer

Introduction

The tumor suppressor gene *Hypermethylated in Cancer 1 (HIC1)* is inactivated by CpG island hypermethylation in a variety of human cancers (Wales *et al.*, 1995). *HIC1* resides in a region of chromosome 17p13 frequently targeted for allelic loss in human cancer (Wales *et al.*,

1995). This region is also associated with the Miller–Dieker Syndrome, a congenital disorder characterized by severe facial and neurologic deficits (Carter *et al.*, 2000; Chen *et al.*, 2003). Homozygous deletion of *Hic1* in mice results in major developmental defects and embryonic lethality (Carter *et al.*, 2000). *HIC1* heterozygous mice retaining one allele of *Hic1*, develop age- and gender-dependent tumors associated with promoter hypermethylation and gene silencing of the remaining wild type (WT) *HIC1* allele (Chen *et al.*, 2003, 2004; Briggs *et al.*, 2008). These studies suggest that *Hic1* has important roles both in development and tumor suppression.

Mutations in the *adenomatous polyposis coli (APC)* gene have been implicated both in familial as well as sporadic gastrointestinal (GI) cancers. *APC* mutations are associated with autosomal dominant inheritance of disease in humans. Similarly, mice that contain a single mutant *Apc* gene encoding a protein truncated at amino acid residue 716 (*Apc*^{Δ716}) develop multiple polyps throughout the GI tract as early as 4 weeks after birth (Oshima *et al.*, 1995; Wu *et al.*, 2009). A major function of APC in human cells is to regulate Wnt signaling in stem cells and cancer by preventing the nuclear translocation of β-catenin (reviewed in (Gregorieff and Clevers, 2005; Reya and Clevers, 2005)). As expected, polyps derived from mice with a disruption in *Apc* function (*Apc*^{min} and *Apc*^{Δ716}), display nuclear β-catenin, typically associated with dysregulated Wnt signaling (Su *et al.*, 1992; Oshima *et al.*, 1995).

Hic1 is a sequence-specific transcriptional repressor with an N-terminal POZ domain, and five C₂H₂ zinc-fingers at the C-terminus (Deltour *et al.*, 1998, 1999, 2002). A growing body of evidence suggests that one important function of *HIC1* is to inhibit the canonical Wnt signaling pathway. Recent studies in mammalian cell lines suggest that *HIC1* antagonizes Wnt signaling through association with TCF4 and β-catenin in a transcriptionally inactive complex retained in the nucleus (Valenta *et al.*, 2006). Moreover, our previous studies have shown that knockdown of *SIRT1*, an important repressive target of *HIC1* (Chen *et al.*, 2005), in breast and colon cancer cells leads to the reactivation of the epigenetically silenced Wnt antagonists, sFRPs (Pruitt *et al.*, 2006). Together, these data suggest that *Hic1* can also fine-tune the Wnt pathway in cancer cells.

Correspondence: Dr SB Baylin, Oncology, Johns Hopkins University School of Medicine, 1650 Orleans Street, CRB I 541, Baltimore, MD 21231, USA.

E-mail: sbaylin@jhmi.edu

⁴These authors contributed equally to this work.

Received 21 August 2010; revised 15 December 2010; accepted 15 December 2010; published online 7 February 2011

We now report that loss of a single *Hic1* allele can promote crypt hyperplasia of the small intestine and further potentiate polyp formation in *Apc*^{+/ Δ 716} mice. *Hic1*^{+/-}, *Apc*^{+/ Δ 716} double heterozygous (DH) mice develop increased numbers of polyps throughout the GI tract by 60 days. *Hic1* is not expressed in polyps with an increase in DNA, and immunohistochemical analyses of polyps show increases in markers such as β -catenin, Sirt1 and Sox9, indicating aberrant Wnt and *Hic1* signaling. Together, our data suggest that loss of a gene frequently silenced via epigenetic mechanisms, *Hic1*, can cooperate with loss of a gene often mutated in GI cancer, *Apc*, to promote tumorigenesis in an *in vivo* model of multiple intestinal neoplasia.

Results

DH mice develop increased numbers of polyps throughout the GI tract

Loss of a single *Hic1* allele complements loss of *Apc* function to promote acceleration of polyp formation in 60-day-old *Hic1*^{+/-}, *Apc*^{+/-} mice. In all four genotypes generated from the cross between *Hic1*^{+/-} females and *Apc*^{+/ Δ 716} male mice, the greatest numbers of polyps in both the small (Figures 1a and d) and large (Figures 1b and d) intestines were present in the GI tracts of DH mice. At this age, no polyps were detected in *Hic1*^{+/-} mice, and WT controls do not develop polyps at any age studied. *Hic1*^{+/-} mice do, however, develop a few polyps by 90 days of age, but the number of tumors is greater in *Apc*^{+/ Δ 716} and DH mice (Supplementary Figure S1). At 60 days, the majority of polyps in *Apc*^{+/ Δ 716} mice were found in the small intestine, as reported previously (Oshima *et al.*, 1995), and the size is predominantly small (<2 mm) (Figures 2a–d). DH mice, however, develop increased numbers of polyps throughout all regions of the small and large intestine (Figures 2a–d). Notably, in the large intestine, there were several large polyps over 2 and 3 mm in DH, with none greater than 3 mm in the single *Apc*^{+/ Δ 716} (Figure 2d). This involvement of the colon is more reminiscent of the spectrum of human GI cancers.

Sirt1 and Hic1 expression are inverse to one another in normal GI tissue

Immunohistochemical analyses reveal that in WT mice *Hic1* expression is largely restricted to the stromal and inflammatory cells in lamina propria in the small intestine, with only occasional nuclear staining in epithelial cells (Figure 3a). By real-time PCR analysis of *Hic1* expression within the small intestine, within some variability in levels, values were not statistically different for WT and *Hic1*^{+/-} mice (Figure 3e). However, there is a statistically significant change in terms of decreased *Hic1* expression in DH mice (Figure 3e). In the colon, by immunohistochemistry, *Hic1* is highly visible in cells in the upper crypt and intercrypt table containing more mature epithelial cells (Figure 3b), whereas it is low to undetectable near the base of the

colonic crypts, where progenitor cells reside (Ponder *et al.*, 1985; Barker *et al.*, 2008, 2009).

In this above setting, we examined the distribution of nuclear Sirt1, a transcription repression target of *Hic1* (Chen *et al.*, 2005). In the small intestine, the protein is expressed throughout the progenitor crypt regions and mature villus epithelial cells (Figure 3c). In *Hic1*^{+/-} mice and DH mice, which have only one functional copy of *Hic1*, the distribution of Sirt1 remains unchanged, but there is a distinct increase in the intensity of Sirt1 staining throughout the crypt and mature villus epithelial region. A much more striking inverse pattern for *Hic1* and Sirt1 is observed in normal mouse colon mucosa. *Hic1* expression in the large intestine is highest in WT animals, whereas the lowest expression appears to be restricted to mice that have only one functional allele of *Hic1* (*Hic1*^{+/-} and DH) (Figure 3b). Furthermore, in the WT mice, *Hic1* expression is inverse to that of Sirt1, which is more restricted to colonic basal crypt regions, and its expression gradually decreases as cells migrate toward the upper crypt, where the cells express *Hic1* (Figure 3d). Inverse to the decreased *Hic1* expression in mice with one functional *Hic1* allele, Sirt1 expression throughout the large intestine appears to have regionally expanded to the more mature cells above the upper crypt in *Hic1*^{+/-} and DH mice (Figures 3b and d). Together, these data suggest that *Hic1* and Sirt1 maintain an inverse relationship in the GI tract and, notably, that the reduction in *Hic1* expression in the GI tract of *Hic1*^{+/-} and DH mice conveys a functional consequence for Sirt1 distribution in this tissue.

Hic1 methylation in normal and neoplastic tissue

In previous settings, loss of *Hic1* expression in tumors in *Hic1*^{+/-} mice, and in many human tumors (Fujii *et al.*, 1998; Dong *et al.*, 2001), has been associated with DNA hypermethylation of either an upstream (*Hic1a*) or downstream (*Hic1b*) promoter region (Chen *et al.*, 2003). Both regions are associated with exons, which are transcribed (Guerardel *et al.*, 2001), and hypermethylation of either can correlate with complete loss of transcripts for the gene (Chen *et al.*, 2003; Briggs *et al.*, 2008). As detailed in the earlier studies, bisulfite sequence analysis can distinguish the WT *Hic1b* region from the targeted allele, but cannot separate WT *Hic1a* from the disrupted allele (Chen *et al.*, 2003; Briggs *et al.*, 2008). To elucidate whether methylation may have a role in the reduced *Hic1* expression in the small and large intestine, as described, or in the increased polyps observed in DH animals, we assessed the methylation status of *Hic1* in the current study using bisulfite sequence analysis, as described previously (Chen *et al.*, 2003; Briggs *et al.*, 2008). Although the overall density of methylation is not dramatic, we do observe the greatest increase in methylation for *Hic1a*, both in polyps from the small and large intestine of DH mice relative to WT animals as well as *Apc*^{+/ Δ 716} (Figures 4a and b). Interestingly, normal small intestine from *Hic1*^{+/-} as well as from DH animals also displays greater methylation relative to WT animals (Figure 4b),

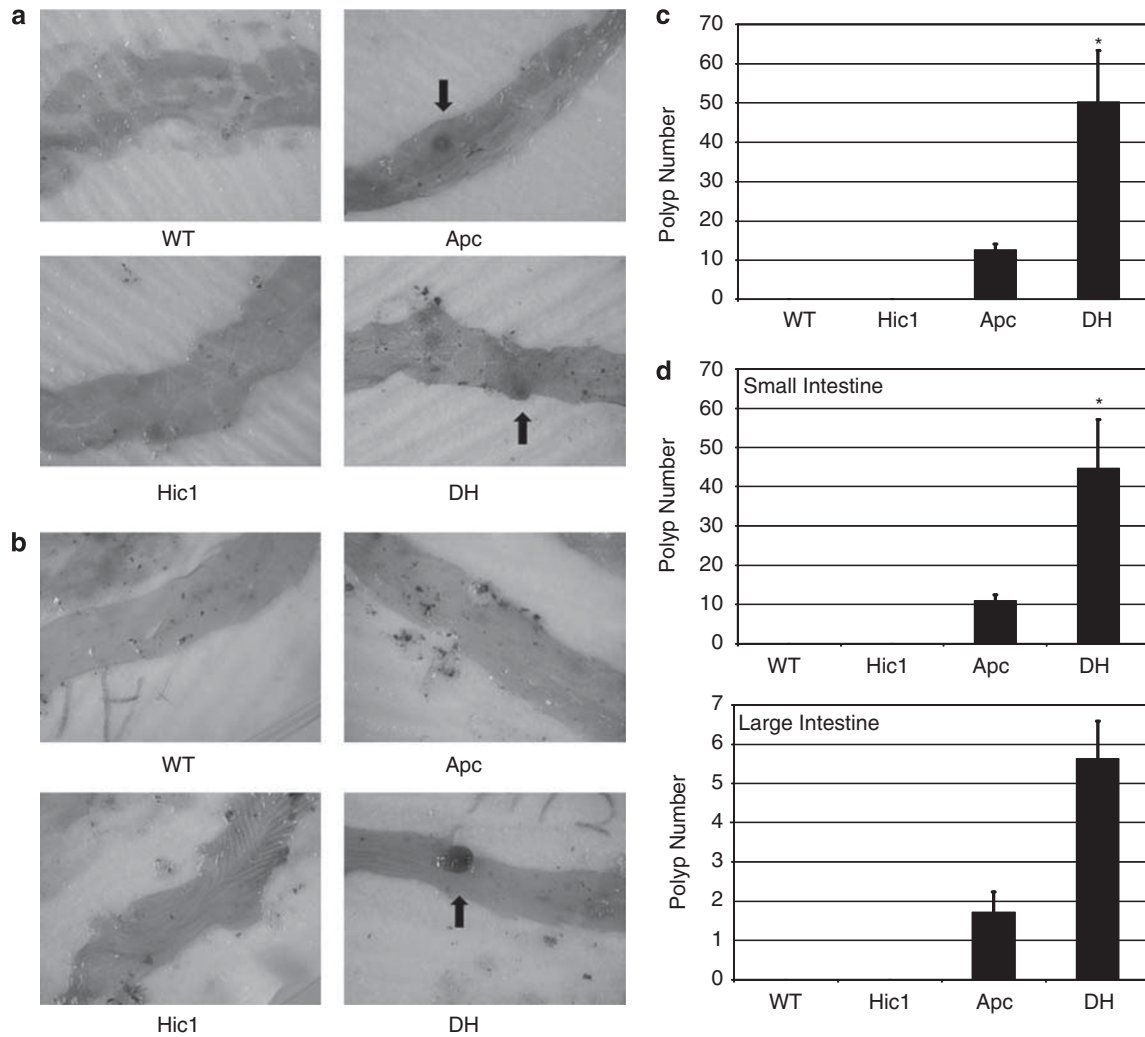


Figure 1 DH mice develop more polyps than Apc mice. (a) Methylene blue staining of intestinal sprays collected from small intestines of WT, *Apc*^{+/ Δ 716} (Apc), *Hic1*^{+/-} (Hic1), and DH *Apc*^{+/ Δ 716}, *Hic1*^{+/-} (DH) mice at 60 days. Sample sizes were as follows: WT, *n* = 12; Hic1, *n* = 13; Apc, *n* = 7; DH, *n* = 8. Arrows indicate polyps. (b) Methylene blue staining of intestinal sprays collected from large intestines of WT, Apc, Hic1 and DH mice at 60 days. Arrows indicate polyps. (c) Values represent the mean number of polyps \pm s.e.m. throughout the entire GI tract as counted under a dissection microscope. (d) Values represent the mean number of polyps \pm s.e.m. in the small or large intestine as indicated. Statistics were carried out as detailed in materials and methods. Comparisons were considered statistically significant at a **P*-value <0.05.

corresponding to the decreased expression observed by real-time PCR (Figure 3e). The WT *Hic1b* region, however, is variably more methylated than *Hic1a* in both the normal small and large intestines in mice of all genotypes (Figures 4c and d). As noted above, there is minimal detectable expression of *Hic1* (Figure 3a) in normal small intestine, but this low level appears to be further reduced in the DH animals (Figure 3e).

Hic1 heterozygotes develop crypt hyperplasia

Despite the lack of significant *Hic1* expression in the small intestine, it remains clear that the genetic loss of a single *Hic1* allele potentiates polyp development. A key finding that may provide some additional insight into the acceleration of polyps in DH mice within the small intestine emerged when we analyzed the proliferation status of the GI tract. Ki67, a hallmark of proliferation, (Barnard *et al.*, 1987), was positive in all polyps

examined (data not shown) and, as expected, restricted to the more proliferative cells in the normal intestinal crypts (Figure 5a). Interestingly, the loss of a single *Hic1* allele leads to crypt hyperplasia. This hyperplasia manifests, in *Hic1*^{+/-} and DH mice, as increased numbers of crypts per villi (Figures 5a and b). No obvious changes in the total number of villi were observed. These hyperplastic crypts have little or no *Hic1*, whereas *Sirt1* expression is abundant (Figure 3). We examined crypts from all genotypes for potential alterations in the progenitor cell marker, *Lgr5* (Barker *et al.*, 2007), and found similar numbers of *Lgr5* positive cells, suggesting no direct effect of *Hic1* allelic loss on this sub-population within each crypt unit (data not shown). However, we did find features associated with crypt dysplasia (Hao *et al.*, 2005) in *Hic1*^{+/-} small intestines (Supplementary Figure S2), as well as a small number of polyps (Supplementary Figure S1). This

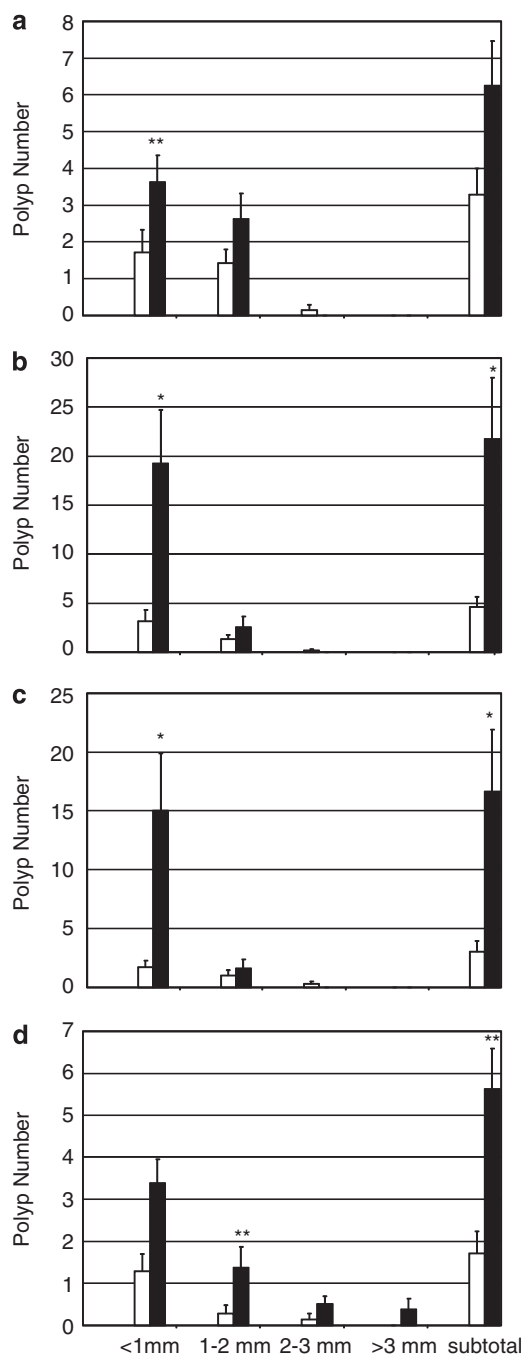


Figure 2 DH mice have more polyps of all sizes in all regions of the GI tract. (a) Values represent the mean number of polyps \pm s.e.m. throughout the proximal small intestine or duodenum counted at 60 days. Polyp size ranges are as indicated. White and black columns indicate *Apc*^{+/Δ716} and DH (respectively). (b) Values represent the mean number of polyps \pm s.e.m. throughout the medial small intestine or jejunum. Polyp size ranges are as indicated. White and black columns indicate *Apc* and DH (respectively). (c) Values represent the mean number of polyps \pm s.e.m. throughout the distal small intestine or ileum. Polyp size ranges are as indicated. White and black columns indicate *Apc* and DH (respectively). (d) Values represent the mean number of polyps \pm s.e.m. throughout the large intestine or colon. Polyp size ranges are as indicated. White and black columns indicate *Apc* and DH (respectively). Statistics were carried out as detailed in materials and methods. Comparisons were considered statistically significant at a **P*-value <0.05 or ***P*-value <0.1.

suggests that the loss of *Hic1* alone may be significant in the development of GI tumors at this early age and, as previously observed, in much older animals as well (Chen *et al.*, 2003).

Polyps do not express Hic1 and display hallmarks of aberrant Hic1 and Wnt signaling

As expected, based on the increase in methylation observed for *Hic1a* in both the large and small intestine (Figure 4) and the absence of *Hic1* expression in normal small intestine, polyps from *Hic1*^{+/-} and DH mice did not express detectable *Hic1* (Figure 6a). Small intestine polyps from *Apc*^{+/Δ716} also did not express *Hic1* (Figure 6a). In the normal and neoplastic tissue from *Apc*^{+/Δ716} mice, however, this may be due to a chromatin-based repressive mechanism surrounding the *Hic1a* region, as there was no increase in DNA methylation for this genotype (Figure 4). *Apc*^{+/Δ716} polyps and tumors from DH mice showed nuclear β -catenin, a hallmark of increased Wnt signaling (Polakis, 2000) (Figure 6a). Interestingly, polyps from *Hic1*^{+/-} mice also contained nuclear β -catenin, suggesting that Wnt signaling is also hyperactive in the neoplasms from this genotype (Figure 6a).

As polyps derived from *Hic1*^{+/-}, *Apc*^{+/Δ716} and DH mice had no detectable *Hic1* expression, we next examined polyps expression of known transcriptional repression targets of *Hic1*. As described previously (Chen *et al.*, 2005) and above, *Sirt1* expression is inversely related to the presence of *Hic1* in normal GI. We find that, concordant with the absence of *Hic1*, *Sirt1* expression is retained in polyps across all genotypes (Figure 6a).

We further extended our analysis to *Sox9*, reported as having reduced gene expression in a microarray screen following *Hic1* overexpression in U2OS osteosarcoma cells (Van Rechem *et al.*, 2009). *Sox9* is a transcription factor found in Paneth cells as well as progenitor cells in intestinal crypts (Bastide *et al.*, 2007). As the above array data was not verified or characterized, we first validated that *Sox9* is truly a *Hic1* target gene and that this relationship exists in the GI. As analyzed by immunohistochemistry, *Sox9* expression, similar to *Sirt1* in normal large intestine, is inverse to the distribution of *Hic1* (Supplementary Figure S3). This protein is also restricted to the nuclei of crypt cells and decreases in more mature cells that express *Hic1*. Also, like *Sirt1*, *Sox9* was highly expressed in all polyps from *Hic1*^{+/-}, *Apc*^{+/Δ716} and DH mice coupled with the absence of *Hic1* expression (Figure 6d). Analysis of the sequence provided by the UCSC genome browser revealed the presence of several potential *Hic1*-binding sites (Pinte *et al.*, 2004; Chen *et al.*, 2005) upstream of the *SOX9* transcriptional start site. *Sox9* expression was increased by greater than twofold in knockout *Hic1*^{-/-} MEFs (Figure 6b). Additionally, *SOX9* was repressed upon ectopic overexpression of *Hic1* in HCT116 human colon cancer cells that do not express endogenous *Hic1* (Figure 6c). Chromatin immunoprecipitation (ChIP) of the ectopically expressed protein to several of the sequence-binding regions for *Hic1* upstream of the

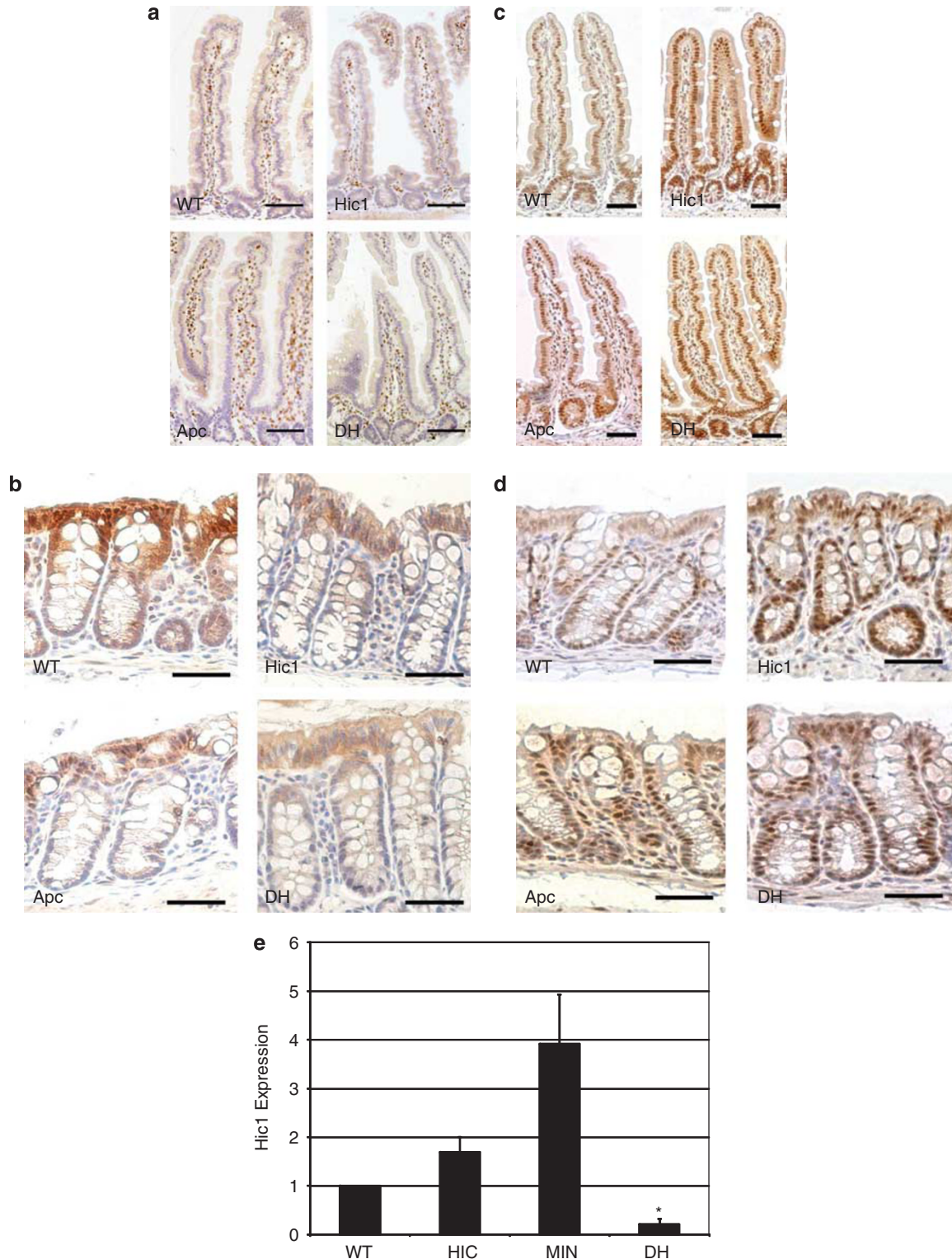


Figure 3 Hic1 and Sirt1 expression throughout the GI tract. **(a)** Hic1 immunohistochemistry of paraffin-embedded small intestine sections from mice as indicated. **(b)** Hic1 immunohistochemistry of paraffin-embedded large intestine sections. **(c)** Sirt1 immunohistochemistry of paraffin-embedded small intestine. **(d)** Sirt1 immunohistochemistry of paraffin-embedded large intestine. Genotypes of mice are as indicated for all panels. Scale bar = 50 μ m for all panels. **(e)** Realtime PCR expression of Hic1 in small intestine. Values represent the mean fold change \pm s.e.m. for triplicates relative to actin. Genotypes of animals are as indicated. Tissue was analyzed from two WT animals, three Hic1, three Min and three DH (* P <0.05).

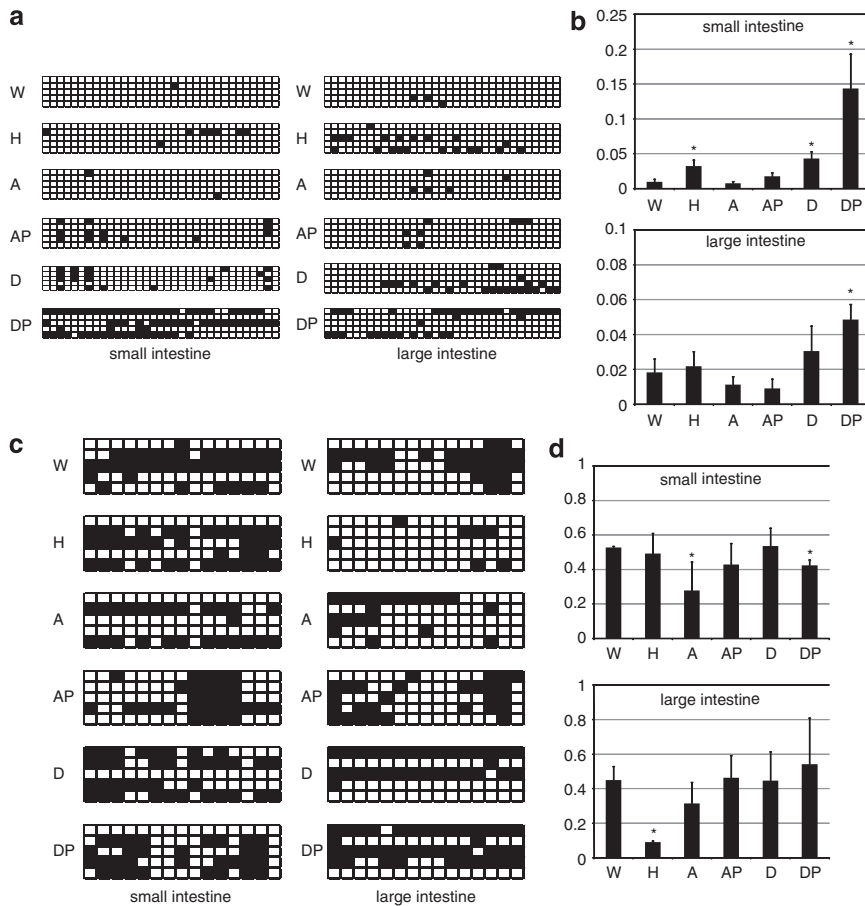


Figure 4 Hic1 methylation analysis by bisulfite sequencing. (a) Left panel: representative alleles for *Hic1a* for bisulfite sequencing of DNA from normal small intestine and small intestine polyps. Each square along a horizontal row = a CpG site in a TA cloned allele with white = unmethylated and black = methylated. Alleles are from non-polyp DNA from WT (W), *Hic1*^{+/-} (H), *Apc*^{+/ Δ 716} (A), polyps from *Apc*^{+/ Δ 716} (AP), non-polyp DH mice (D) and DH polyps (DP), respectively. Right panel: shown are representative alleles for *Hic1a* in normal large intestine and large intestine polyp DNA (right) with alleles listed as for left panel. (b) Percent methylation (Y-axis), with bars = \pm s.e.m., per alleles shown in A and, on the X axis, 1 = W, 2 = H, 3 = A, 4 = AP, 5 = D and 6 = DP. An average of 68 alleles was sequenced for each genotype. (c) Representative alleles for *Hic1b* bisulfite sequencing in the small intestine (left), and large intestine (right), respectively, with allele symbols as in A. (d) Percent methylation per allele for *Hic1b* with axes and symbols exactly as in B. For all graphs: **P* < 0.05 relative to WT. An average of 20 alleles was sequenced for each genotype.

SOX9 gene correlated with this finding (Supplementary Figure S4).

Discussion

In the current study, we have established a mouse model in which loss of function for *Hic1* augments the role of *Apc* loss for development of GI tumors. Importantly, this effect of *Hic1* loss of function accentuates not only the tumorigenesis in the small intestine, which dominates in *Apc*^{+/ Δ 716} mice, but also increases both the number and size of polyps in the large intestine. These results are consistent with our previous work, indicating that *Hic1* can serve a tumor-suppressive function through a variety of important mechanisms involving its role for transcriptional repression of multiple downstream targets (Carter *et al.*, 2000; Chen *et al.*, 2003, 2004; Briggs *et al.*, 2008).

The role of *Hic1* in the above model may be to provide a cellular setting that provides *Apc* loss an optimal opportunity for exerting an oncogenic stimulus. Recently, Clevers *et al.* have shown that loss of *Apc* in mouse intestine is most tumorigenic when engineered to target intestinal stem cells (Barker *et al.*, 2009). The loss of one *Hic1* allele appears to increase the number of stem cell-containing crypt cell compartments and lead to some dysplastic features in these regions. This scenario may thus increase the target cell population susceptible to the oncogenic effects of *Apc* disruption. Presumably, this setting may favor the addition of intestinal stem cells to increased Wnt pathway activity driven by loss of *Apc* function. Interestingly, *Hic1*^{+/-} mice also develop polyps (Supplementary Figure S1), and spontaneous GI cancers appear in older *Hic1*^{+/-} animals (Chen *et al.*, 2003), suggesting that the crypt hyperplasia and dysplasia are significant even without the additional genetic contribution from *Apc*^{+/ Δ 716}.

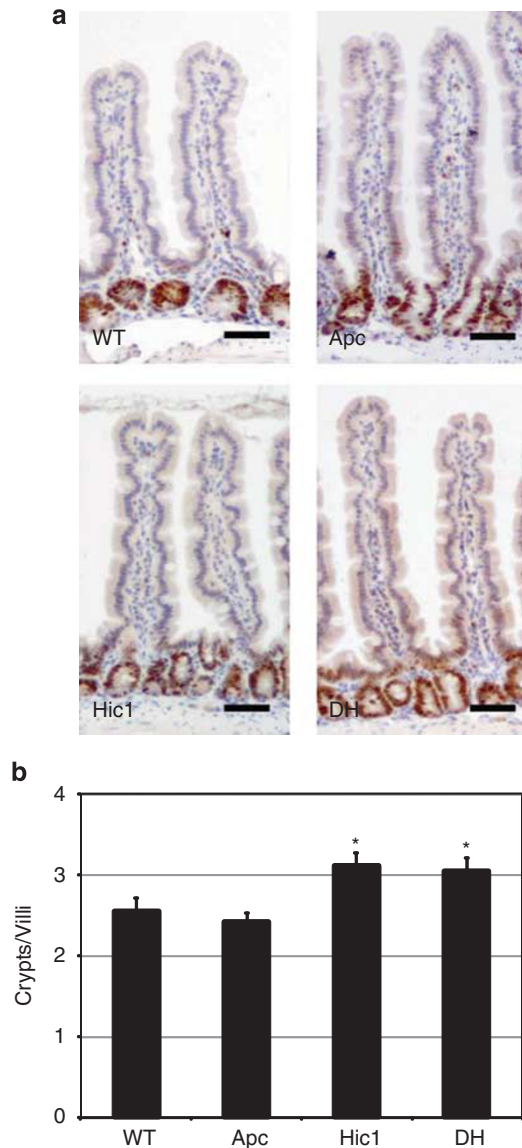


Figure 5 Hic1 heterozygous mice develop crypt hyperplasia of the small intestine. (a) Shown are sections from small intestine stained with an antibody against Ki67 for mice as indicated. Scale bar = 50 μ m. (b) The number of crypts and villi per field were counted by two independent observers. Nine fields from three animals within each genotype were used in counting. Values represent the mean number of crypts per villi \pm s.e.m. in the small intestine. Asterisks indicate $P < 0.05$ by Student's *t*-test.

Hic1 is not only a critical developmental protein, but is emblematic, for human cancers, of a tumor suppressor gene for which loss of function arises through epigenetic rather than genetic alterations (Wales *et al.*, 1995). Loss of Hic1 expression in colon cancer, specifically, has also been associated with silencing associated with DNA hypermethylation (Nosho *et al.*, 2009) (Maekawa *et al.*, 2001). In the particular mouse model described here, the mechanism for the silencing of the remaining WT allele of Hic1 in tumors is not yet as clear as in previous studies of our Hic1 heterozygous mice (Chen *et al.*, 2003; Briggs *et al.*, 2008). In our earlier work,

dense methylation of the proximal promoter of the WT allele of the gene has almost always been present in the different tumor types that arise in these mice alone, or when they are crossed with other tumor-prone mice (Chen *et al.*, 2004; Briggs *et al.*, 2008). In the present case, the increases we find in tumors for Hic1 promoter DNA methylation are quite small in both promoter regions studied. Although these changes may still be significant for loss of gene transcription, they accompany other chromatin changes that aid in gene silencing.

Another puzzling feature for expression of Hic1 in our model is the difference between normal small and large intestine. In the latter, a clear pattern is present, wherein Hic1 is expressed in the more differentiated cells of the more luminal region, whereas, interestingly, the transcriptional repression targets we studied, Sirt1 and Sox 9, are expressed in the stem cell-containing crypt regions. These latter proteins seem to lose this regional distribution in the Hic1 heterozygous mice, consistent with a modulatory role for Hic1 in their expression patterns. However, despite the clear crypt region changes we observe in the small intestine of the Hic1^{+/-} mice, Hic1 protein expression is below detection by immunohistochemistry in the epithelial cells. However, there is a reduction in Hic1 mRNA expression in DH animals by real-time PCR. Thus, we suspect that a small amount of protein may be functional in this region, because loss of a single WT Hic1 allele affects the number of small intestine crypts, causing some changes in Sirt1 and Sox9 expression patterns, and clearly complements tumorigenicity in the DH animals.

Previous studies from others, as well as our work, have identified a number of relevant targets of Hic1 in a variety of biological contexts. In the cerebellum of mice, loss of this protein leads to increased levels of the downstream repression target gene, *Atonal Homolog 1*. These changes complement loss of the Sonic Hedgehog receptor, *PATCHED*, to increase the numbers of progenitor cells and augment cerebellar tumorigenesis (Briggs *et al.*, 2008). Hic1 loss also associates with spatial disruption of the downstream repression target, ephrin A1 (Zhang *et al.*, 2010), which is a key patterning morphogen in development. However, in our present model, the molecular mechanisms by which Hic1 loss exerts changes in the intestine are not yet clear. As we show, two known repression target genes of Hic1, Sirt1 (Chen *et al.*, 2005) and Sox9 (Van Rechem *et al.*, 2009) are both highly expressed in nuclei of tumor cells in the Hic1^{+/-}, Apc^{+/-} mice. Sirt1, a mammalian ortholog of the yeast Sir2 protein, is a direct transcriptional target of Hic1 (Chen *et al.*, 2005). The role for Sirt1 in tumorigenesis has proven substantially complex to understand as both Sirt1 knockout and overexpression systems have yielded discordant results. A study in which Sirt1 knockout animals were crossed to Apc^{min/+} mice showed that loss of Sirt1 had no effect on polyp number in Apc^{min/+} animals, but that polyp size was decreased (Boily *et al.*, 2009). These data suggest a pro-tumorigenic role for Sirt1 in this system. Additional work has recently linked Sirt1 to repression of the Wnt

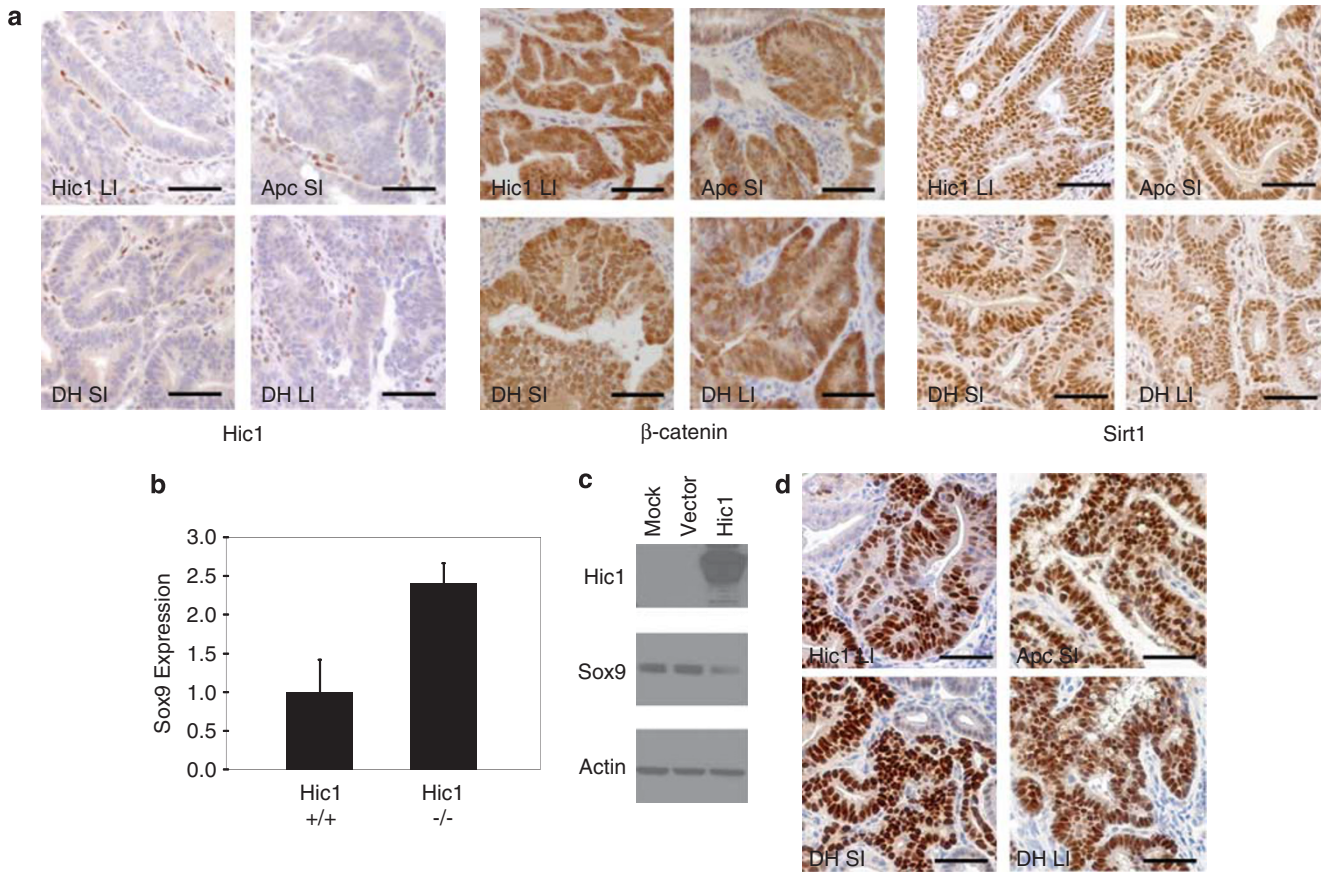


Figure 6 Polyps display hallmarks of aberrant hic and wnt signaling. (a) Immunohistochemistry of paraffin-embedded polyps from small intestine (SI) and large intestine (LI) for antibodies as indicated. Genotypes of mice are as indicated. Scale bar = 50 μ m. (b) Real-time PCR expression for Sox9 in MEFs. Values represent the mean fold change \pm s.e.m. for triplicates. Genotypes of cells are as indicated. (c) Shown are western blot analyses of protein lysates from HCT116 cells transfected for 48 h with cDNA as indicated. (d) Immunohistochemistry using an antibody against Sox9 for paraffin-embedded polyps from small intestine (SI) and large intestine (LI). Genotypes of mice are as indicated. Scale bar = 50 μ m.

inhibitors, disheveled, providing an additional Wnt-related mechanism by which Sirt1 may promote tumorigenesis (Holloway *et al.*, 2010). However, another study showed the opposite effect, in that polyps were decreased in *Apc^{min/+}* animals upon overexpression of Sirt1 in the intestine (Firestein *et al.*, 2008). Although the role for Sirt1 in GI tumor initiation and progression may remain controversial, in our current study, significant Sirt1 expression is present in all polyps and inversely correlates with Hic1 expression. Thus, either the protein has an oncogenic role in this setting or, if it is a tumor suppressor, it is ineffectual because of lack of signaling to downstream targets.

Sox9 has been shown to be repressed by greater than threefold in U2OS osteosarcoma cells infected with Ad-HIC1 (Van Rechem *et al.*, 2009). In this regard, we now confirm Sox9 as a direct Hic1 target gene for transcriptional repression in human colon cancer cells and mouse MEFs by both expression analysis and ChIP. This high-mobility group box transcription factor has been described in the GI tract as a Wnt pathway target (Blache *et al.*, 2004) and, thus, this gene may be co-regulated by both Hic1 and Wnt signaling. Sox9 expression appears to positively correlate with β -catenin

expression in human colorectal cancer (Lu *et al.*, 2008). A recent study also showed that SOX9 represses expression of protein kinase C alpha in proliferating intestinal epithelial cells (Dupasquier *et al.*, 2009), a gene that, in *Apc^{min/+}* mice, may provide a protective role against intestinal tumorigenesis (Oster and Leitges, 2006). Sox9 serves as an important crypt-related transcription factor through its ability to repress genes associated with differentiation (Blache *et al.*, 2004), and an imbalance in Sox9 expression gives rise to crypt dysplasia (Bastide *et al.*, 2007). This may be tightly tied to our current finding that crypt hyperplasia is coupled with crypt dysplasia in our Hic1^{+/-} mice.

In summary, we describe, in a mouse model, an oncogenic interaction between loss of function for the *Hic1* and *Apc* genes. This complementation appears fueled by increases in crypt cell regions due to the *Hic1* disruption. We associate increases in two Hic1 transcriptional repression targets, *Sirt1* and *Sox9*, with changes in the above model, but their direct roles remain to be defined for the tumorigenic events studied. Our mouse model will prove extremely valuable for exploring this and other questions linking Hic1 and the Wnt pathway to intestinal tumorigenesis.

Materials and methods

Mice

Mice were housed in a pathogen-free environment and observed daily for signs of ill health. *Hic1*^{+/-} females were crossed to *Apc*^{+/ Δ 716} males to generate mice used in the studies described. Both strains were backcrossed as described previously (Oshima *et al.*, 1995; Chen *et al.*, 2003; Briggs *et al.*, 2008) and maintained in a C57BL/6 background. Genotyping was performed as described previously (Oshima *et al.*, 1995; Carter *et al.*, 2000).

Polyp counts

Mice were killed at 60 or 90 days by CO₂ asphyxiation. The intestinal tract was removed, opened longitudinally and washed with PBS, as described previously (Moser *et al.*, 1990). The cleared tissue was fixed in 10% buffered formalin and subsequently stained with 1.5% methylene blue in physiological saline (0.9%). Intestines were destained with 10% ethanol using several changes of fresh destaining solution to attain the desired level of stain. At this level, intestinal tissue appeared light blue with significantly darker polyps. The proximal, medial and distal regions of the small intestine and the entire large intestine were examined. Polyps were scored with a dissecting microscope by at least two independent observers, and the average counts were further analyzed. Student's *t*-test was used to compare the mean allele count between DH and *Apc* for 60 days by anatomical regions and subregions. All comparisons were considered statistically significant at a *P*-value <0.05 (*) or *P*-value <0.1 (**). All statistical analyses were performed using Stata 10 statistical package.

Immunohistochemistry

Hic1 immunohistochemistry was performed as previously described (Chen *et al.*, 2003). Antigen retrieval for deparaffinized tissue sections was performed in citrate buffer (small intestine) or Tris-EDTA buffer (colon) for 20 min by using a steamer. Following blocking of endogenous peroxidase, paraffin-embedded sections were submitted to immunohistochemistry using the Vectastain Elite ABC system (Vector Laboratories, Burlingame, CA, USA). Citrate buffer antigen retrieval and Vectastain ABC kits (Vector Laboratories) were used for all other immunohistochemistry. The following antibodies were used: Sox9 (Chemicon, Billerica, MA, USA), β -Catenin (BD Transduction Laboratories, Sparks, MD, USA), Ki67 (Novocastra Laboratories, Newcastle upon Tyne, UK) and Sirt1 (Upstate Biotechnology, Billerica, MA, USA).

Crypt counting

Ki67 staining was used to mark crypt cells within sections prepared, as described above. Images were collected at $\times 20$ magnification throughout the small intestine, and at least 21 fields from 4 mice across all genotypes were utilized. Crypt hyperplasia was documented by counting crypts as described previously with some modification (Stuber *et al.*, 1998; Boivin *et al.*, 2003). In the current study, the number of crypts and intestinal villi were counted for each image by two independent observers, and the average of the two counts was used in the data analysis.

Bisulfite sequencing

Genomic DNA extraction and bisulfite modification, and sequencing of tissue derived from WT, *Hic1*^{+/-}, *Apc*^{+/ Δ 716} and DH mice was performed as previously described (Frommer

et al., 1992; Chen *et al.*, 2003). Primers used were within *Hic1a* and *1b* promoters as previously described (Chen *et al.*, 2003). Sequences are available upon request. An average of 68 alleles was sequenced for each genotype for *Hic1a*, whereas an average of 20 alleles for each was analyzed for *Hic1b*. Weighted means were generated and statistical analyses performed are as follows: the generalized estimating equation data analysis, assuming independent correlation structure with robust standard error estimates and Gaussian distribution was used to calculate the mean percent methylation per allele, and corresponding standard errors for each genotype. To control for multiple testing, Sidak adjustment method was used to correct for family-wise error rate. All statistical analyses were performed using Stata version 10 statistical package and are shown in Supplementary Table 2.

Preparation of MEFs

MEFs from E10.5 mouse embryos were prepared as described previously (Briggs *et al.*, 2008). Early passage (p2) MEFs were seeded at a density of 2×10^5 per well in a six-well plate. The cells were maintained in DMEM (Cellgro, Manassas, VA, USA) supplemented with 10% bovine calf serum (HyClone, Hudson, NH, USA) and antibiotics, and grown at 37°C in 5% CO₂ atmosphere.

RNA preparation and real-time analysis

Total RNA was isolated from cell pellets and DNase 1 treated using RNeasy (Qiagen, Valencia, CA, USA). Real-time PCR was performed using conditions and primers described previously, including initial normalization to GAPDH.

Cell culture

Cell lines were maintained according to ATCC guidelines. All transfections were performed using Lipofectamine 2000 (Invitrogen, Carlsbad, CA, USA), according to manufacturer's instructions.

Western analysis

Antibodies used were: Sox9 (Chemicon) and V5 (Invitrogen). β -Actin (Sigma, St Louis, MO, USA) was used as a loading control.

ChIP

ChIP was carried out on HCT116 cells transfected as described above. ChIP was performed as described previously (McGarvey *et al.*, 2006) using V5 antibody (Invitrogen) or IgG control (Millipore, Billerica, MA, USA).

Conflict of interest

The authors declare no conflict of interest.

Acknowledgements

We thank Guosheng Liu for technical assistance with dissection, Kimberly Briggs for primers, Robert Beatty for assistance with *Hic1*^{+/-} breeding and Kathy Bender for manuscript submission. This work was supported by grants from the National Cancer Institute CA043318 (SBB), National Institutes of Environmental Health Sciences ES015226 and ES011858 (SBB). Additional support was provided by the American Cancer Society (HM and WZ).

References

- Barker N, Ridgway RA, van Es JH, van de Wetering M, Begthel H, van den Born M *et al.* (2009). Crypt stem cells as the cells-of-origin of intestinal cancer. *Nature* **457**: 608–611.
- Barker N, van de Wetering M, Clevers H. (2008). The intestinal stem cell. *Genes Dev* **22**: 1856–1864.
- Barker N, van Es JH, Kuipers J, Kujala P, van den Born M, Cozijnsen M *et al.* (2007). Identification of stem cells in small intestine and colon by marker gene *Lgr5*. *Nature* **449**: 1003–1007.
- Barnard NJ, Hall PA, Lemoine NR, Kadar N. (1987). Proliferative index in breast carcinoma determined in situ by Ki67 immunostaining and its relationship to clinical and pathological variables. *J Pathol* **152**: 287–295.
- Bastide P, Darido C, Pannequin J, Kist R, Robine S, Marty-Double C *et al.* (2007). Sox9 regulates cell proliferation and is required for Paneth cell differentiation in the intestinal epithelium. *J Cell Biol* **178**: 635–648.
- Blache P, van de Wetering M, Duluc I, Domon C, Berta P, Freund JN *et al.* (2004). SOX9 is an intestine crypt transcription factor, is regulated by the Wnt pathway, and represses the CDX2 and MUC2 genes. *J Cell Biol* **166**: 37–47.
- Boily G, He XH, Pearce B, Jardine K, McBurney MW. (2009). SirT1-null mice develop tumors at normal rates but are poorly protected by resveratrol. *Oncogene* **28**: 2882–2893.
- Boivin GP, Washington K, Yang K, Ward JM, Pretlow TP, Russell R *et al.* (2003). Pathology of mouse models of intestinal cancer: consensus report and recommendations. *Gastroenterology* **124**: 762–777.
- Briggs KJ, Corcoran-Schwartz IM, Zhang W, Harcke T, Devereux WL, Baylin SB *et al.* (2008). Cooperation between the Hic1 and Ptch1 tumor suppressors in medulloblastoma. *Genes Dev* **22**: 770–785.
- Carter MG, Johns MA, Zeng X, Zhou L, Zink MC, Mankowski JL *et al.* (2000). Mice deficient in the candidate tumor suppressor gene Hic1 exhibit developmental defects of structures affected in the Miller-Dieker syndrome. *Hum Mol Genet* **9**: 413–419.
- Chen W, Cooper TK, Zahnow CA, Overholtzer M, Zhao Z, Ladanyi M *et al.* (2004). Epigenetic and genetic loss of Hic1 function accentuates the role of p53 in tumorigenesis. *Cancer Cell* **6**: 387–398.
- Chen WY, Wang DH, Yen RC, Luo J, Gu W, Baylin SB. (2005). Tumor suppressor HIC1 directly regulates SIRT1 to modulate p53-dependent DNA-damage responses. *Cell* **123**: 437–448.
- Chen WY, Zeng X, Carter MG, Morrell CN, Chiu Yen RW, Esteller M *et al.* (2003). Heterozygous disruption of Hic1 predisposes mice to a gender-dependent spectrum of malignant tumors. *Nat Genet* **33**: 197–202.
- Deltour S, Guerardel C, Leprince D. (1999). Recruitment of SMRT/N-CoR-mSin3A-HDAC-repressing complexes is not a general mechanism for BTB/POZ transcriptional repressors: the case of HIC-1 and gammaFDP-B. *Proc Natl Acad Sci USA* **96**: 14831–14836.
- Deltour S, Guerardel C, Stehelin D, Leprince D. (1998). The carboxy-terminal end of the candidate tumor suppressor gene HIC-1 is phylogenetically conserved. *Biochim Biophys Acta* **1443**: 230–232.
- Deltour S, Pinte S, Guerardel C, Wasylyk B, Leprince D. (2002). The human candidate tumor suppressor gene HIC1 recruits CtBP through a degenerate GLDLSKK motif. *Mol Cell Biol* **22**: 4890–4901.
- Dong SM, Kim HS, Rha SH, Sidransky D. (2001). Promoter hypermethylation of multiple genes in carcinoma of the uterine cervix. *Clin Cancer Res* **7**: 1982–1986.
- Dupasquier S, Abdel-Samad R, Glazer RI, Bastide P, Jay P, Joubert D *et al.* (2009). A new mechanism of SOX9 action to regulate PKCalpha expression in the intestine epithelium. *J Cell Sci* **122**: 2191–2196.
- Firestein R, Blander G, Michan S, Oberdoerffer P, Ogino S, Campbell J *et al.* (2008). The SIRT1 deacetylase suppresses intestinal tumorigenesis and colon cancer growth. *PLoS One* **3**: e2020.
- Frommer M, McDonald LE, Millar DS, Collis CM, Watt F, Grigg GW *et al.* (1992). A genomic sequencing protocol that yields a positive display of 5-methylcytosine residues in individual DNA strands. *Proc Natl Acad Sci USA* **89**: 1827–1831.
- Fujii H, Biel MA, Zhou W, Weitzman SA, Baylin SB, Gabrielson E. (1998). Methylation of the HIC-1 candidate tumor suppressor gene in human breast cancer. *Oncogene* **16**: 2159–2164.
- Gregorieff A, Clevers H. (2005). Wnt signaling in the intestinal epithelium: from endoderm to cancer. *Genes Dev* **19**: 877–890.
- Guerardel C, Deltour S, Pinte S, Monte D, Begue A, Godwin AK *et al.* (2001). Identification in the human candidate tumor suppressor gene HIC-1 of a new major alternative TATA-less promoter positively regulated by p53. *J Biol Chem* **276**: 3078–3089.
- Hao LY, Armanios M, Strong MA, Karim B, Feldser DM, Huso D *et al.* (2005). Short telomeres, even in the presence of telomerase, limit tissue renewal capacity. *Cell* **123**: 1121–1131.
- Holloway KR, Calhoun TN, Saxena M, Metoyer CF, Kandler EF, Rivera CA *et al.* (2010). SIRT1 regulates Dishevelled proteins and promotes transient and constitutive Wnt signaling. *Proc Natl Acad Sci USA* **107**: 9216–9221.
- Lu B, Fang Y, Xu J, Wang L, Xu F, Xu E *et al.* (2008). Analysis of SOX9 expression in colorectal cancer. *Am J Clin Pathol* **130**: 897–904.
- Maekawa M, Sugano K, Ushiyama M, Fukayama N, Nomoto K, Kashiwabara H *et al.* (2001). Heterogeneity of DNA methylation status analyzed by bisulfite-PCR-SSCP and correlation with clinicopathological characteristics in colorectal cancer. *Clin Chem Lab Med* **39**: 121–128.
- McGarvey KM, Fahrner JA, Greene E, Martens J, Jenuwein T, Baylin SB. (2006). Silenced tumor suppressor genes reactivated by DNA demethylation do not return to a fully euchromatic chromatin state. *Cancer Res* **66**: 3541–3549.
- Moser AR, Pitot HC, Dove WF. (1990). A dominant mutation that predisposes to multiple intestinal neoplasia in the mouse. *Science* **247**: 322–324.
- Nosho K, Kure S, Irahara N, Shima K, Baba Y, Spiegelman D *et al.* (2009). A prospective cohort study shows unique epigenetic, genetic, and prognostic features of synchronous colorectal cancers. *Gastroenterology* **137**: 1609–1620 e1-3.
- Oshima M, Oshima H, Kitagawa K, Kobayashi M, Itakura C, Taketo M. (1995). Loss of Apc heterozygosity and abnormal tissue building in nascent intestinal polyps in mice carrying a truncated Apc gene. *Proc Natl Acad Sci USA* **92**: 4482–4486.
- Oster H, Leitges M. (2006). Protein kinase C alpha but not PKCzeta suppresses intestinal tumor formation in ApcMin/+ mice. *Cancer Res* **66**: 6955–6963.
- Pinte S, Stankovic-Valentin N, Deltour S, Rood BR, Guerardel C, Leprince D. (2004). The tumor suppressor gene HIC1 (hypermethylated in cancer 1) is a sequence-specific transcriptional repressor: definition of its consensus binding sequence and analysis of its DNA binding and repressive properties. *J Biol Chem* **279**: 38313–38324.
- Polakis P. (2000). Wnt signaling and cancer. *Genes Dev* **14**: 1837–1851.
- Ponder BA, Schmidt GH, Wilkinson MM, Wood MJ, Monk M, Reid A. (1985). Derivation of mouse intestinal crypts from single progenitor cells. *Nature* **313**: 689–691.
- Pruitt K, Zinn RL, Ohm JE, McGarvey KM, Kang SH, Watkins DN *et al.* (2006). Inhibition of SIRT1 reactivates silenced cancer genes without loss of promoter DNA hypermethylation. *PLoS Genet* **2**: 344–352.
- Reya T, Clevers H. (2005). Wnt signalling in stem cells and cancer. *Nature* **434**: 843–850.
- Stuber E, Von Freier A, Marinescu D, Folsch UR. (1998). Involvement of OX40-OX40L interactions in the intestinal manifestations of the murine acute graft-versus-host disease. *Gastroenterology* **115**: 1205–1215.

Su LK, Kinzler KW, Vogelstein B, Preisinger AC, Moser AR, Luongo C *et al.* (1992). Multiple intestinal neoplasia caused by a mutation in the murine homolog of the APC gene. *Science* **256**: 668–670.

Valenta T, Lukas J, Doubravska L, Fafulek B, Korinek V. (2006). HIC1 attenuates Wnt signaling by recruitment of TCF-4 and beta-catenin to the nuclear bodies. *Embo J* **25**: 2326–2337.

Van Rechem C, Rood BR, Touka M, Pinte S, Jenal M, Guerardel C *et al.* (2009). Scavenger chemokine (CXC motif) receptor 7 (CXCR7) is a direct target gene of HIC1 (hypermethylated in cancer 1). *J Biol Chem* **284**: 20927–20935.

Wales MM, Biel MA, el Deiry W, Nelkin BD, Issa JP, Cavenee WK *et al.* (1995). p53 activates expression of HIC-1, a new candidate tumour suppressor gene on 17p13.3. *Nat Med* **1**: 570–577.

Wu S, Rhee KJ, Albesiano E, Rabizadeh S, Wu X, Yen HR *et al.* (2009). A human colonic commensal promotes colon tumorigenesis via activation of T helper type 17T cell responses. *Nat Med* **15**: 1016–1022.

Zhang W, Zeng X, Briggs KJ, Beaty R, Simons B, Chiu Yen RW *et al.* (2010). A potential tumor suppressor role for Hic1 in breast cancer through transcriptional repression of ephrin-A1. *Oncogene* **29**: 2467–2476.



This work is licensed under the Creative Commons Attribution-NonCommercial-No Derivative Works 3.0 Unported License. To view a copy of this license, visit <http://creativecommons.org/licenses/by-nc-nd/3.0/>

Supplementary Information accompanies the paper on the Oncogene website (<http://www.nature.com/onc>)